ELSEVIER

Journal of Nuclear Materials 283–287 (2000) 152–156

journal of nuclear materials

www.elsevier.nl/locate/jnucmat

Sink effect of grain boundary on radiation-induced segregation in austenitic stainless steel

S. Watanabe [a,*], Y. Takamatsu [b], N. Sakaguchi [b], H. Takahashi [b]

[a] *Advanced Materials Laboratory, Department of Materials Science, Faculty of Engineering, Hokkaido University, Kita-13, Nishi-8, Kita-ku, Sapporo 060-8628, Japan*

[b] *Center for Advanced Research of Energy Technology, Hokkaido University Kita-13, Nishi-8, Kita-ku, Sapporo 060-8628, Japan*

Abstract

We have investigated the orientation dependence of grain boundaries in radiation-induced segregation (RIS) in an austenitic stainless steel under irradiation using a high-voltage electron microscope (HVEM) at the Hokkaido University HVEM facility and a new rate equation model for RIS, which incorporates the grain boundary sink strength for point defects. The $\langle 1\,1\,0\rangle$ tilt grain boundaries were chosen for the present study. It was observed that, after electron irradiation at a dose rate of 2.0×10^{-3} dpa s^{-1} to 10 dpa at temperatures of either 623 or 723 K, RIS was enhanced as the tilt angle increased but was suppressed at coincidence grain boundaries ($\Sigma 9$ and $\Sigma 3$). The present result indicates that one needs to explicitly consider the grain boundary sink strength as an important factor affecting radiation-induced grain boundary phenomena (RIGBPH). This work can be thought as a study of the radiation-induced grain boundary phenomena associated with grain boundary engineering related to non-equilibrium phenomena.

1. Introduction

Radiation-induced segregation (RIS) near grain boundaries is known to cause a significant degradation in the physical, chemical and mechanical properties of austenitic stainless steels [1,2]. Radiation-induced phenomena are known to be closely related to the point defects introduced due to collision between high-energy particles and atoms in an alloy. The grain boundary is the one of places where complex phenomena occur since it is a strong point defect sink. Although there is a relatively large body of studies on the effect of grain boundary character on equilibrium segregation [3–5] or thermally induced precipitation [6,7], such information on radiation-induced grain boundary phenomena (RIGBPH) is very scarce (see, for e.g., [8]).

In the present study we have, for the first time, substantially investigated the effect of grain boundary character on RIS. We carried out an electron irradiation experiment for an austenitic stainless steel (Fe–15Cr–20Ni) using a high-voltage electron microscope (HVEM-H1300) at the Hokkaido University HVEM facility. A newly developed rate equation model for intergranular RIS, which was developed previously [9] and modified in the present work, has been used to evaluate the grain boundary sink efficiency for point defects. The present paper focuses on the sink effect of grain boundary character on RIS. We will show that the assumption of the so-called ''perfect sink condition'', which is a boundary condition that all the point defects generated by irradiation diminish completely at the grain boundary and has customarily been used in the theoretical evaluations, e.g., [9], is generally invalid except for some random grain boundaries.

2. Experiment

An Fe–Cr–Ni alloy containing 20.8Ni, 14.5Cr and, as impurities, 0.003C, 0.01Si and 0.003P (in wt.%) was prepared. After cold rolling to 150 μm followed by heat

* Corresponding author. Tel.: +81-11 706 6770; fax: +81-11 706 6772.

E-mail address: watanabe@loam-ms.eng.hokudai.ac.jp (S. Watanabe).

0022-3115/00/$ - see front matter
PII: S0022-3115(00)00204-X

treatment at 1323 K for 60 m and electro-polishing, TEM foil specimens were irradiated with 1 MeV electrons at various temperatures using a HVEM (H-1300) at the Hokkaido University. The mean damage rate was 2.0×10^{-3} dpa s^{-1}. The irradiation temperatures were 623 and 723 K and the dose, up to 10 dpa. The $\langle 1\,1\,0\rangle$ tilt grain boundaries, which have their rotation axis in parallel to the boundary with the tilt angles up to 70.5°, were chosen for irradiation. Since the present work used polycrystalline specimens with a few tens of micrometer grain size, the available misorientated grain boundaries were limited to certain kinds of tilt boundaries. These grain boundaries studied include small angle tilt boundaries, $\Sigma 3$ and $\Sigma 9$ coincidence boundaries and random boundaries. After irradiation, we carried out ion-thinning for the TEM specimens with an ion-milling instrument (GATAN: DuoMill Model 600) for a few minutes, in order to remove surface regions of a few hundred nanometers. Chemical composition was then measured using a field-emission-type analytical 200 keV transmission electron microscope (JEOL: JEM-2010F) equipped with an energy dispersive X-ray analyzer (Noran: Voyager 2000-EDS).

3. The model and calculation method

The calculations performed to evaluate the rate equations for the solvent atom (Fe), solute atom (Cr and Ni) and point defect (vacancy and interstitial) concentrations for various irradiation conditions used a model developed previously [9]. The approach is based on solving the coupled diffusion equations for vacancies, interstitials and solvent and solute atoms to provide the terms which couple the defect and atom fluxes. We dealt with the inverse-Kirkendall flux by taking account of interstitial diffusion, which is well known as the mixed-dumbbell mechanism, as well as vacancy diffusion [10,11]. In the calculation, we also considered the spatial resolution in the EDS analysis with a finite-size probe by averaging the calculated concentration profile using the formula of the normalized two-dimensional Gaussian average for the one-dimensional concentration profile [9]. The probe radius used in averaging was 1 nm for FE-TEM [12,13]. The last technique is necessary for simulating the actual profile data obtained by TEM-EDS analysis [12–14].

The continuity equations used for the quantities of interest are

$$\frac{\partial C_k}{\partial t} = -\nabla \cdot \boldsymbol{J}_k \quad (k \text{ denotes solvent Fe, solute Cr and Ni}), \tag{1}$$

$$\frac{\partial C_\mathrm{v}}{\partial t} = -\nabla \cdot \boldsymbol{J}_\mathrm{v} + \eta G_\mathrm{dpa} - K_\mathrm{vi}(D_\mathrm{i} + D_\mathrm{v})C_\mathrm{v}C_\mathrm{i} - S_\mathrm{i}D_\mathrm{i}(C_\mathrm{v} - C_\mathrm{v}^\mathrm{eq}), \tag{2}$$

$$\frac{\partial C_\mathrm{i}}{\partial t} = -\nabla \cdot \boldsymbol{J}_\mathrm{i} + \eta G_\mathrm{dpa} - K_\mathrm{vi}(D_\mathrm{i} + D_\mathrm{v})C_\mathrm{v}C_\mathrm{i} - S_\mathrm{i}D_\mathrm{i}C_\mathrm{i}, \tag{3}$$

where C_k is the concentration of k-atoms, C_v and C_i are the concentration of vacancies and interstitials, C_v^eq is the equilibrium vacancy concentration at a given temperature, $\boldsymbol{J}_k$ is the flux of k-atoms, $\boldsymbol{J}_\mathrm{v}$ and $\boldsymbol{J}_\mathrm{i}$ are the fluxes of vacancy and interstitials, C_v^eq is the damage efficiency (1 in the case of electron irradiation), G_dpa is the generation rate of point defects by irradiation, K_vi is the recombination rate of point defects and D_v and D_i are the diffusivity of vacancies and interstitials, respectively.

The rate equations (1)–(3) were evaluated as functions of the one-dimensional coordinate perpendicular to the grain boundary and of the irradiation time. The main parameters used in the calculation are available in [9]. In this study, we additionally defined the sink strength of the grain boundary as

$$S^\mathrm{GB} = A \sin\frac{\theta}{2}, \tag{4}$$

where A is a parameter in units of the inverse square of the length and θ is the tilt angle. S^GB can be obtained considering the edge dislocations, which are sink sources for point defects, presumably to be aligned at a tilt grain boundary, and A is then written as $2Z/(bd)$. Here b is the magnitude of the Burger's vector of edge dislocation (i.e., $a_0/2\ \langle 1\,1\,0\rangle$, where a_0 is the lattice constant), d the inter-plane distance along the dislocation and Z is an enhancement factor. Z/d then gives the number of extinguished point defects on the dislocation per unit length. We used (4) as a boundary condition instead of 'the perfect sink condition'. The latter condition means that all the point defects generated by irradiation are annihilated completely at the grain boundary, and this has customarily been used as a boundary condition (e.g., [9]). In the present study, we set $Z/d = 3/a_0$. This gives A to about 10^{20} m^{-2}.

4. Results and discussion

Examples of the effect of grain boundary misorientation on RIS are shown in Figs. 1(a) and (b), which represent concentration profiles near a small angle tilt grain boundary (tile angle: 3.5°) and a random grain boundary (tilt angle 64°), respectively, after electron irradiation for both areas with the same conditions to a dose of 3 dpa at 723 K. Unfilled circles and squares are the experimental data of Ni and Cr concentrations, respectively, and the solid lines indicate computer simulation results. The deviations between the data points and the solid line in the matrix area in Fig. 1(a) are probably due to EDS counting statistics. It can be seen that the RIS at a small angle tilt boundary was

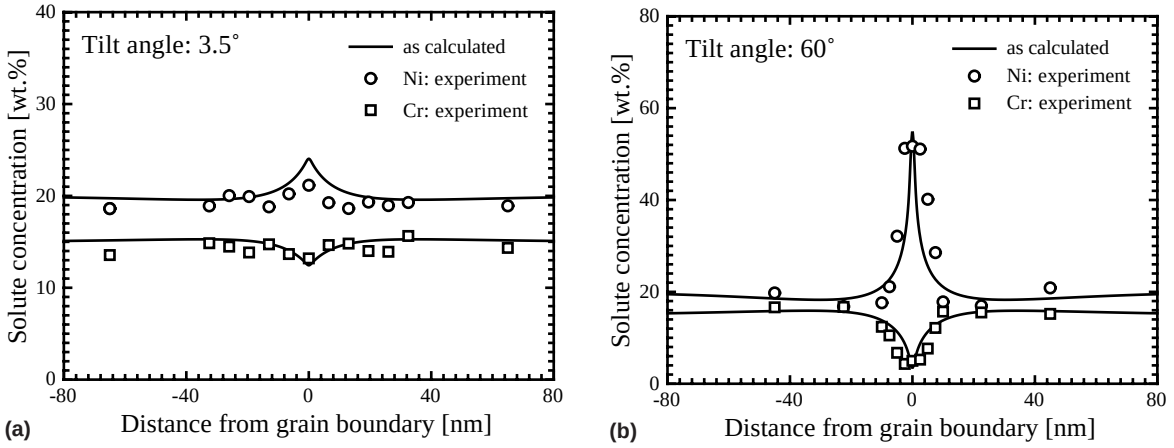

Fig. 1. RIS at two different grain boundaries after electron irradiation to 3 dpa at 723 K: (a) a small angle tilt grain boundary ($\theta = 3.5°$) (b) a random grain boundary ($\theta = 60°$); solid lines are theoretical predictions and unfilled characters are experimental data.

remarkably suppressed but not so at a random grain boundary. Since RIS is caused due to point defect flow to a sink, the sink strength for point defects for a random boundary is much stronger than the strength at a coherent and/or a low-energy grain boundary like a small angle tilt grain. In Eq. (4), the grain boundary sink strength, S^{GB}, becomes stronger as the tilt angle increases. This is consistent with the above argument and, in fact, the theoretical results in Fig. 1 show a good agreement with the experimental data for both types of grain boundaries. Exceptions exist, however, in the cases of the coincidence grains with low Σ values at higher tilt angles, because Eq. (4) does not explicitly include the grain boundary energy. Discussion on theoretical considerations for these special boundaries will be given later.

The dose dependence up to 10 dpa on RIS for a random grain boundary is shown in Fig. 2(a) and that for a twin boundary, ($\Sigma 3$), in Fig. 2(b). Fig. 2(a) well reproduced the theoretical dose dependence on intergranular RIS, which was predicted in Fig. 4 of [9] with an assumption of the perfect sink condition, while that for a twin boundary in Fig. 2(b) showed almost no RIS up to 3 dpa followed by a gradual increase in RIS. This means that the boundary has not worked as a sink for point defects until about 3 dpa and then starts working as a sink with higher dose. The detailed mechanism of the sink effect change in the latter case is not known yet.

Fig. 3 shows the misorientation dependence of intergranular RIS after irradiated to 3 dpa at 723 K as a function of the tilt angle, θ, from $\langle 1\,1\,0\rangle$. It is evident that intergranular RIS is suppressed at low sigma boundaries

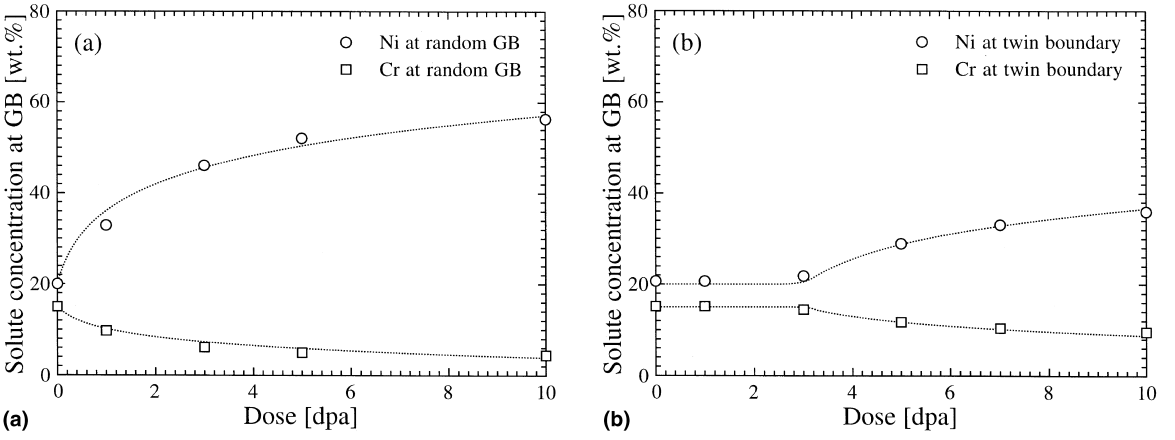

Fig. 2. Dose dependence of RIS at two different grain boundaries by electron irradiation up to 10 dpa at 623 K: (a) at a random grain boundary (b) at a $\{1\,1\,1\}\Sigma 3$ twin boundary.

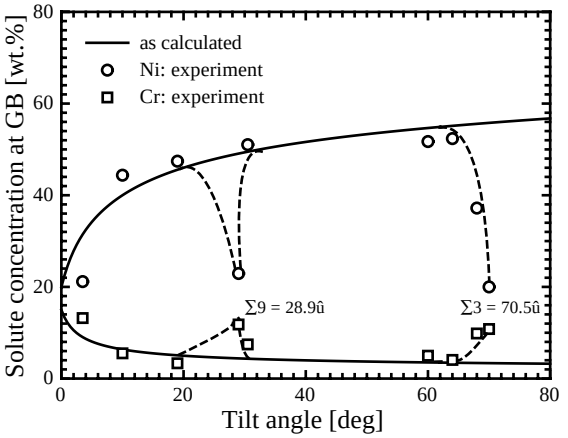

Fig. 3. The tilt angle dependence of RIS at various grain boundaries after electron irradiation to 3 dpa at 723 K; the rotation axis is ⟨1 1 0⟩ for all grains; solid lines are theoretical prediction in terms of Eq. (4) and unfilled characters are experimental data.

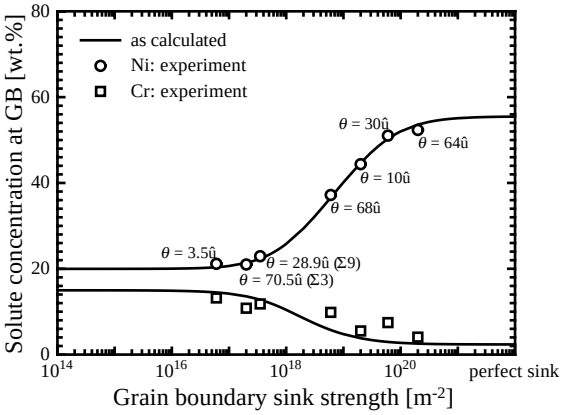

Fig. 4. Theoretical prediction (lines) of RIS (3 dpa at 723 K) vs. grain boundary sink strength, S^{GB}; the experimental RIS results (unfilled characters) for various kinds of grains are superimposed.

of 28.9°/Σ9 and 70.5°/Σ3 and a 3.5°/Σ1 small angle grain boundary. Except near these 'special boundaries' RIS significantly occurred and was enhanced with an increase of the tilt angle. It should be noted that intergranular RIS was more enhanced at a GB with a larger tilt angle, although the Σ values are the same (see data points at 20°/Σ33 and 59°/Σ33). We further carried out measurements on intergranular RIS with a different dose of 1 dpa at 723 K, and also at a different temperature of 623 K with the doses of 1 and 3 dpa. The results showed the same trends of misorientation dependence as shown in Fig. 3, but the intergranular RIS at grain boundaries was more enhanced when the dose or the temperature was higher. An independent evaluation of the sink strength parameter revealed that a larger value of Z/d, i.e., the larger A, causes the enhancement of RIS.

The theoretical results shown by the solid line in Fig. 3 well predicted the experimental results for random grain boundaries. This means that use of the boundary condition in Eq. (4) is appropriate for such non-special grain boundaries. The difference between the experimental datum and the theoretical prediction for the special boundaries, however, indicates that a further consideration should be made for such grain boundaries. According to Brandon [15], the angle range over which the coincidence orientation relationship is maintained depends on the Σ value in the form of $\Sigma^{-1/2}$, so that a grain boundary with the larger Σ value has the narrower deviation angle as a special boundary. Hence, the angular range where the RIS data deviated from the theoretical curve in Fig. 3 can be expected to be narrower for a higher Σ value GB. The grain boundary strength constant, A, should then be defined for each special grain boundary and evaluated separately.

In order to evaluate sink efficiency for non-random grain boundaries, we predicted, in Fig. 4, RIS at a dose of 3 dpa at 723 K as a function of a parameter of grain boundary sink strength, S^{GB}, with the experimental RIS results for various kinds of grains. It is indicated that, in the region of S^{GB} more than 10^{20} m^{-2} (e.g., the point of $\theta = 64°$), the perfect sink condition is considered to be applicable, while that of S^{GB} less than 10^{17} m^{-2} (e.g., the point of $\theta = 3.5°, 70.5°$) has the least sink efficiency. There exists an intermediate region or transient. In other words, an appropriate choice of value of grain boundary sink strength parameter will give a good reproducibility of RIS even for a special boundary.

5. Concluding remarks

We have investigated the effect of grain boundary misorientation on radiation-induced segregation (RIS), introducing a new parameter for the grain boundary sink strength. The present result clearly indicates that one needs to consider the grain boundary nature as an important factor affecting intergranular RIS and also other RIGBPHs. A false conclusion may be drawn if one implicitly assumes the perfect sink condition for a non-random grain boundary and ignores the allowable misorientation range for theoretical prediction of intergranular RIS.

Acknowledgements

This work has been supported by the Ministry of Education, grant-in-aid for EYS (#11750564) and by the Kazato foundation.

References

[1] J.F. Bate, R.W. Powell, E.R. Gilbert, in: D. Kramer, H.R. Brager, J.S. Perrin (Eds.), Proceedings of the 10th Conference on Effects of Radiation on Materials, ASTM STP 725, American Society for Testing and Materials, Philadelphia, PA, 1980, p. 713.
[2] L.K. Mansur, K. Farrell, J. Nucl. Mater. 170 (1990) 236.
[3] T. Watanabe, S. Kitamura, S. Karashima, Acta Metall. 28 (1980) 455.
[4] B.D. Powell, D.P. Woodruff, Philos. Mag. 34 (1976) 169.
[5] P. Lejcek, Anal. Chim. Acta 297 (1994) 165.
[6] B. Forest, M. Biscondi, Metall. Sci. 12 (1978) 202.
[7] J. Lecoze, M. Biscondi, J. Levy, C. Goux, Mem. Sci. Rev. Metall. 70 (1973) 397.
[8] H. Takahashi, N. Hashimoto, Mater. Trans. JIM 34 (1993) 1027.
[9] S. Watanabe, N. Sakaguchi, N. Hashimoto, H. Takahashi, J. Nucl. Mater. 224 (1995) 158.
[10] P.R. Okamoto, L.E. Rehn, J. Nucl. Mater. 83 (1979) 2.
[11] R.A. Johnson, N.Q. Lam, Phys. Rev. B 13 (1976) 4364.
[12] K. Nakata, O. Okada, Y. Ueki, T. Kamino, J. Electron Microsc. 47 (1998) 193.
[13] S. Watanabe, N. Sakaguchi, H. Takahashi, J. Nucl. Mater. 232 (1996) 113.
[14] R.G. Faulkner, T.S. Morgan, E.A. Little, X-ray Spectrom. 23 (1994) 195.
[15] D.G. Brandon, Acta Metall. 14 (1966) 1479.